

The evolution of fast-growing coral reef fishes

<https://doi.org/10.1038/s41586-023-06070-z>

Alexandre C. Siqueira^{1,2,4}✉, Helen F. Yan^{1,2,4}, Renato A. Morais^{1,2,3} & David R. Bellwood^{1,2}

Received: 19 August 2022

Accepted: 11 April 2023

Published online: 17 May 2023

 Check for updates

Individual growth is a fundamental life history trait^{1–4}, yet its macroevolutionary trajectories have rarely been investigated for entire animal assemblages. Here we analyse the evolution of growth in a highly diverse vertebrate assemblage—coral reef fishes. We combine state-of-the-art extreme gradient boosted regression trees with phylogenetic comparative methods to detect the timing, number, location and magnitude of shifts in the adaptive regime of somatic growth. We also explored the evolution of the allometric relationship between body size and growth. Our results show that the evolution of fast growth trajectories in reef fishes has been considerably more common than the evolution of slow growth trajectories. Many reef fish lineages shifted towards faster growth and smaller body size evolutionary optima in the Eocene (56–33.9 million years ago), pointing to a major expansion of life history strategies in this Epoch. Of all lineages examined, the small-bodied, high-turnover cryptobenthic fishes shifted most towards extremely high growth optima, even after accounting for body size allometry. These results suggest that the high global temperatures of the Eocene⁵ and subsequent habitat reconfigurations⁶ might have been critical for the rise and retention of the highly productive, high-turnover fish faunas that characterize modern coral reef ecosystems.

Somatic growth—the increase in body tissues during ontogeny—is a fundamental trait that drives animal life history^{1,2}. The variation in somatic growth rates across populations results from the allocation of finite resources to competing life history traits (that is, growth, reproduction and survival) with the goal of maximizing fitness^{2–4,7}. As growth rates are optimized rather than maximized, suites of life history strategies evoking several solutions to the same problem co-evolved with one another and are therefore correlated⁴. These clustered traits place species along a fast–slow axis of variation in life histories, whereby species at one extreme exhibit faster growth and reproductive rates, smaller sizes and earlier ages at maturity compared with species at the slow end of the axis⁸. As a consequence, growth trajectories are intrinsically linked with other life history parameters, most notably with maximum body size⁹. Species tend to grow quickly to a smaller maximum size compared with those that grow slowly to a larger maximum size¹⁰. These composite life history traits (that is, life history traits correlated with other life history traits), such as growth, can therefore be good proxies to characterize a species' life history strategy, which is crucial for ecosystem and population assessments^{1,11,12}.

Life history strategies likely co-evolved in response to local biotic and abiotic conditions^{13,14}. Thus, the evolutionary trajectories of composite life history traits can be indicative of both the underlying processes that shaped past ecosystems and the impacts of these ecosystems on modern taxa. Somatic growth rates have been shown to be relatively plastic between distinct populations of conspecifics, changing in response to the duration of growth seasons^{15,16}, food availability¹³ and predator–prey interactions^{13,17}. As a consequence, large-scale changes in environmental and ecological conditions should be mirrored by the expression of different growth strategies. Coral reefs, which are highly

productive ecosystems, exhibited a substantial compositional change 33.9–5.3 million years ago (Ma) during the Oligocene–Miocene with the diversification of both corals and reef-associated fishes^{6,18,19}. As fishes expanded into new habitats and exploited new food resources, faster life histories arose with the diversification of small, high-turnover reef fishes⁶. Given the disproportionately large energetic contribution of these fishes to modern coral reefs, specifically the cryptobenthic and planktivorous taxa^{20,21}, it appears that the iconic productivity of today's reefs may have arisen, at least in part from the expansion of faster reef fish growth trajectories.

Although many studies have assessed the evolutionary patterns of specific life history trade-offs that included growth³, as well as the evolution of certain growth strategies²², studies addressing the evolution of growth trajectories for an entire animal assemblage are lacking. Here we assess the evolution of growth trajectories across a diverse assemblage of vertebrates displaying a wide range of life histories—coral reef fishes^{23,24}. Despite sharing a common habitat, coral reef fishes span over seven orders of magnitude in body mass²⁵ and therefore exhibit a large diversity of growth trajectories²⁶. Unsurprisingly, growth is a dominant life history trait for fishes and has been used to explain variations in physiological processes¹, large-scale spatial distributions²⁷ and relative extinction risks²⁸. Given its key role for determining the critical ecosystem process and service of biomass production on coral reefs²⁹, we mostly focus our analyses on growth, but we also explore its intrinsic correlation with body size. To assess coral reef fish growth from an evolutionary perspective, we first calculated a standardized, composite metric summarizing growth trajectories at the species level and applied a robust, predictive framework to estimate values for unsampled species. We then used a comparative phylogenetic framework to assess

¹Research Hub for Coral Reef Ecosystem Functions, College of Science and Engineering, James Cook University, Townsville, Queensland, Australia. ²ARC Centre of Excellence for Coral Reef Studies, James Cook University, Townsville, Queensland, Australia. ³Paris Sciences et Lettres Université, École Pratique des Hautes Études, EPHE-UPVD-CNRS, USR 3278 CRIODE, Perpignan, France. ⁴These authors contributed equally: Alexandre C. Siqueira, Helen F. Yan. [✉]e-mail: alexandre.siqueira@my.jcu.edu.au

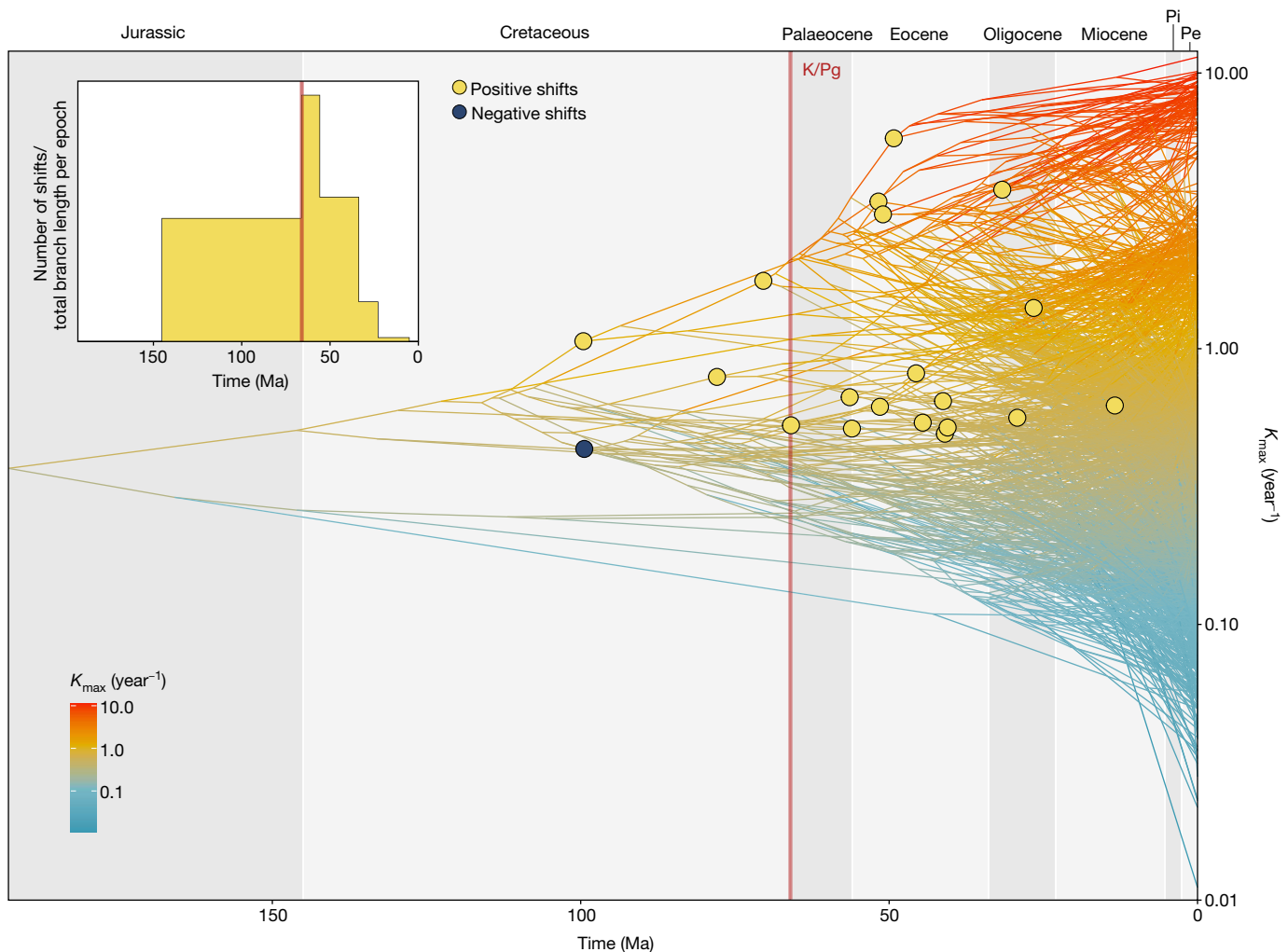


Fig. 1 | Phylogenetic reconstruction of reef fish growth. Standardized growth coefficient (K_{\max}) reconstructed through time across the phylogenetic tree of coral reef-associated fishes ($n = 2,474$). The points represent estimated shifts in the evolutionary regime of growth detected through multi-optima OU models. The light yellow points represent shifts towards higher values of evolutionary optima (faster growth rates), whereas the dark blue point

represents the opposite. Note that the y axis is shown as a \log_{10} scale. Inset: the number of positive shifts divided by the total branch length in the phylogeny per geological epoch (yaxis) through time (x axis). This metric gives an indication of the probability of shifts controlled by the availability of locations for them to occur. The red line represents the K/Pg boundary. Pe, Pleistocene; Pi, Pliocene.

how growth rates and body sizes have evolved through time across coral reef fish lineages. We hypothesize that the evolution of faster life histories would have coincided with the expansion of lineages during the Oligocene–Miocene⁶ and that this was essential for the energetic composition of today's coral reef fish assemblages.

Evolutionary shifts in growth

Our boosted regression tree analysis had a high predictive accuracy and was used to predict the standardized growth coefficient K_{\max} for reef fish species without empirically measured data (Supplementary Results). Derived from the von Bertalanffy growth coefficient K , K_{\max} represents the rate at which individual fishes would reach their asymptotic size if they grew to the maximum reported size for that species²⁶ (unit, year^{-1} ; Methods). By placing K_{\max} values in a phylogenetic context³⁰, we found a notable pattern of regime shifts throughout reef fish evolution. Our multi-optima Ornstein–Uhlenbeck (OU) models³¹ detected 20 evolutionary regime shifts with high confidence (occurring in 75% of posterior samples; Methods) across the reef fish phylogeny. Of the 20 shifts detected, 19 occurred towards higher (faster) growth evolutionary optima, and in only one instance did it shift towards a lower optimum

K_{\max} value (Fig. 1). Using a less conservative threshold of detection (50% of posterior samples), we found two additional shifts towards lower K_{\max} values; however, ten more shifts towards high growth were also identified (Extended Data Fig. 1). In combination with the ancestral state reconstruction (Fig. 1), these results suggest that the evolution of growth coefficients in reef fishes had a strong directionality towards faster growth rates (Extended Data Fig. 2). Although extant species cover a large range of growth coefficient values, evolutionary novelty mainly occurred at the higher end of the spectrum. In other words, departures from the ancestral evolutionary regimes in reef fish growth almost always happened towards faster growth rates.

The timing of evolutionary regime shifts in growth is also disproportionately concentrated, with most occurring in the Eocene (56–33.9 Ma), peaking at about 47 Ma (Fig. 1). When controlling for the total branch length per epoch, we found more positive shifts in the Palaeocene and Eocene (Fig. 1 inset). We also found similar patterns when we used an alternative chronogram³² (Methods), with a higher probability of shifts occurring in the Eocene, despite some shifts being found in more recent times in the Oligocene and Miocene (Extended Data Fig. 3). Notably, in our main analysis, we detected only one shift in the entire Neogene (Miocene, Pliocene and Pleistocene, from 23 Ma to 2.6 Ma) a

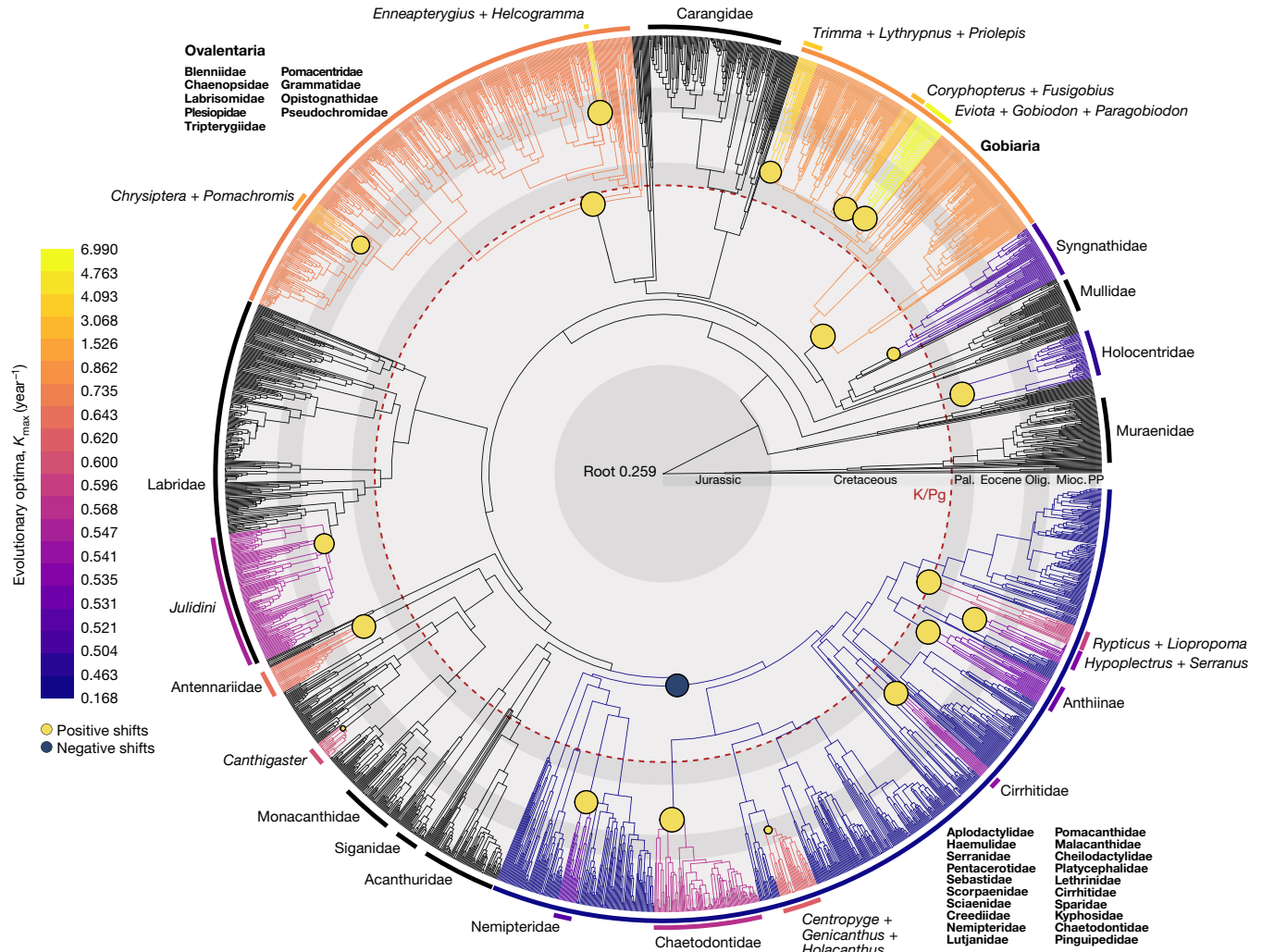


Fig. 2 | The location and magnitude of growth regime shifts in the reef fish phylogeny. Branches and external arcs are discretely coloured according to the estimated value of the median evolutionary optimum in growth that clades shifted towards. The black branches represent lineages without any detectable shift in evolutionary optimum of growth. The points on the nodes represent

the same shifts depicted in Fig. 1; that is, shifts towards higher K_{\max} values (light yellow) and shifts towards a lower K_{\max} values (dark blue). The size of the points is scaled according to the posterior probability of the shift. The red dashed line represents the K/Pg boundary. Mioc., Miocene; Olig., Oligocene; Pal., Palaeocene; PP, Pliocene–Pleistocene.

period in which most lineages appeared and for which the confidence of phylogenetic reconstructions and inference is maximal. There were no detectable changes in the last 13 million years. The only regime shift towards a lower growth optimum in reef fishes was detected well before the Cretaceous–Paleogene (K/Pg, 66 Ma) boundary, at about 100 Ma (Fig. 1).

From a taxonomic perspective, evolutionary regime shifts in growth are spread throughout the reef fish phylogeny. Although some species-rich families, such as Acanthuridae, Labridae (without Julidini), Carangidae and Mullidae, were found to retain the root evolutionary growth regime (Fig. 2), many other speciose groups displayed regime shifts. The oldest shifts occurred at the base of larger clades, such as the Gobiaria (Gobiiformes and Apogonidae), and the crown group that now encompasses typical coral reef families such as Serranidae, Lutjanidae, Chaetodontidae and Pomacanthidae. Notably, this latter evolutionary shift was towards a lower evolutionary optimum growth value. Multiple groups nested within this large, slower-growing clade subsequently exhibited a secondary shift towards a higher growth optima, such as the Chaetodontidae, the Nemipteridae and the Anthiinae serranids (Fig. 2). However, the highest magnitude of change in growth evolutionary trajectories occurred at the base of clades that contain small-bodied, cryptobenthic reef fish groups. Both the Gobiaria and the Ovalentaria

(including Blenniidae, Tripterygiidae and Pomacentridae), presented shifts towards an extremely high median evolutionary optima in K_{\max} (Fig. 2). Subsequent shifts within gobies cumulatively led to the highest growth optimum detected in the reef fish tree, with an over 20-fold estimated increase from the root optimum in the clade containing the genera *Eviota*, *Gobiodon* and *Paragobiodon*.

Shifts in size and allometry

After finding frequent and strong shifts in growth coefficients throughout reef fish evolution, we investigated whether these shifts would also be observed in body size (measured here as maximum body length) and in the allometric scaling relationship between growth and size among species. Our multi-optima OU model using body size revealed an inverse reflection of the growth results (Extended Data Fig. 4), that is, there was an accumulation of shifts towards smaller body sizes in the Eocene, highlighting the inversely correlated nature of these two life history traits. However, in the case of size, we found more shifts towards higher values spread throughout the tree (Extended Data Fig. 4), indicating that not all instances of evolution of larger body sizes were accompanied by the evolution of slower growth rate optima.

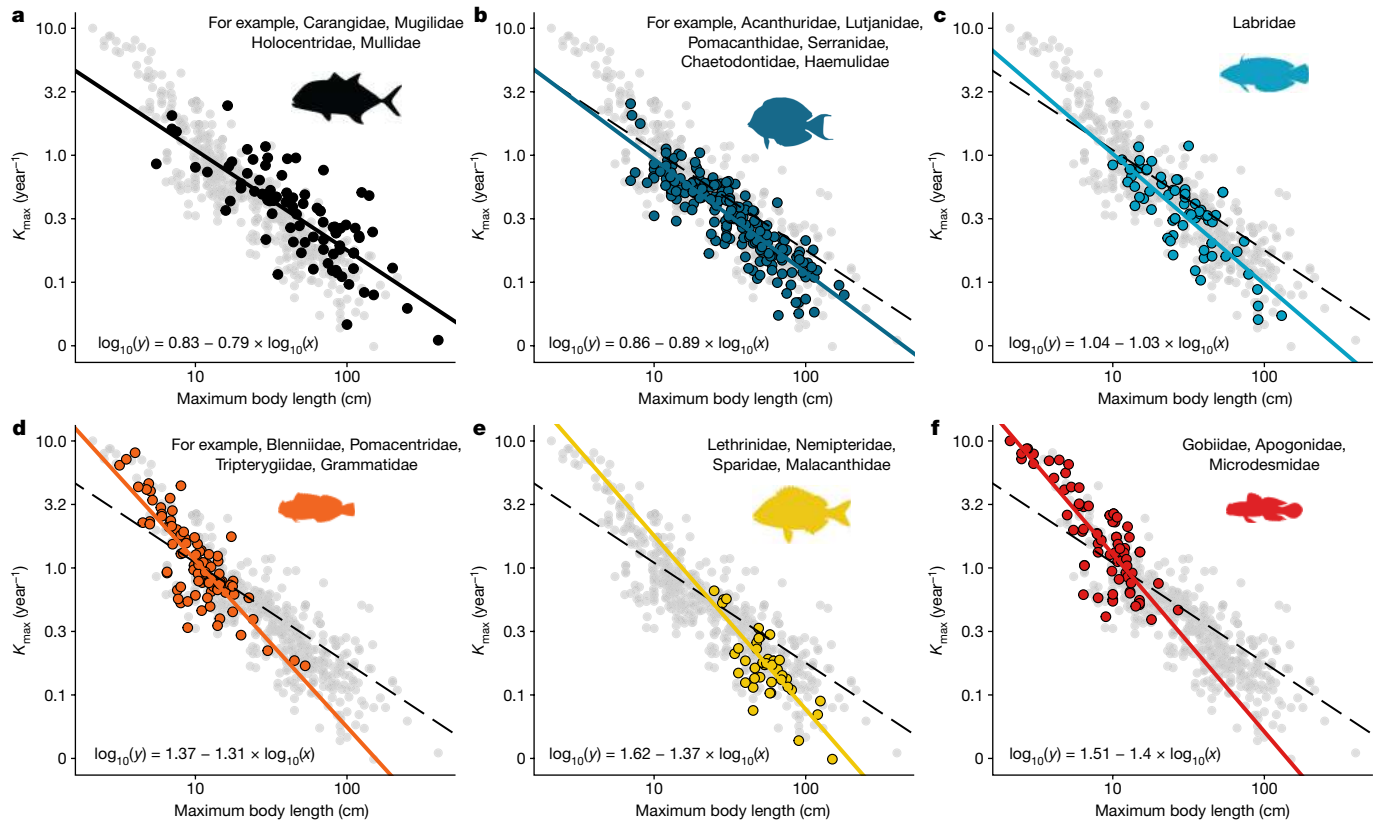


Fig. 3 | Evolutionary regime shifts in the allometry between growth and maximum body length in reef fishes. **a–f**, Reconstructed values (points) of K_{\max} and maximum body length at the most recent common ancestor of each genus ($n = 602$) of the reef fish phylogeny. The black lines (solid in **a**, dashed in **b–f**) represent the root state coefficients for the reef fish tree, estimated by a mixed Gaussian phylogenetic model. For **b–f**, each subsequent panel shows an evolutionary regime shift detected in the relationship between the traits along

the phylogeny, with respective slopes and intercepts (coloured lines), and all tips that display that relationship in the present (coloured points). The panels are organized in order of the steepness of the slopes. The root allometry is shown in **a**, and the other plots show an increase in growth relative to body size (steeper allometry). Both axes are on a \log_{10} scale. The names in each panel refer to extant families that retained that evolutionary regime through time. Fish silhouettes were sourced from fishualize⁵².

To explore the allometric relationship between size and growth, we applied a mixed Gaussian phylogenetic model³³ using the genus-level reef fish phylogeny (Methods). This model detected a total of five evolutionary regime shifts in the allometric growth scaling through time (Extended Data Fig. 5). All regimes were associated with distinct OU models; therefore, each shift had different evolutionary optima for the coefficients of the relationship between growth and size. The root allometric scaling state was retained through time in families like Carangidae, Mugillidae, Holocentridae and Mullidae (Fig. 3a and Extended Data Fig. 5). All subsequent shifts from that root allometry detected by the model represented a steepening of the slope (becoming more negative; Fig. 3b–f). In alignment with the ancestral state reconstruction results, two of the most extreme allometric shifts happened in the main cryptobenthic clades: the Gobiaria (slope = -1.4) and the Ovalearia (slope = -1.31) (Fig. 3d,f). Thus, these two non-related reef fish lineages represent major evolutionary departures from the typical allometry, with species growing substantially faster than predicted by their maximum body length. Notably, although the clade containing the families Lethrinidae, Nemipteridae, Sparidae and Malacanthidae is generally composed of larger-sized species, it has also been identified as having a substantially steep allometry (slope = -1.37) (Fig. 3e).

Discussion

By applying a robust predictive framework within a phylogenetic context, we reveal recurrent departures in life history regimes throughout coral reef fish evolution. Notably, these evolutionary regime shifts

occurred predominantly towards increased growth optima (faster growth trajectories) and smaller body sizes. This suggests either an asymmetrical exploration or selection/retention of these fast life history dynamics in the evolution of reef-associated fish lineages. Although the slower growth trajectory regimes remained relatively constant through time, the high end of the reef fish growth spectrum has been a constant source of evolutionary novelty. As a result, extant coral reef fishes display faster growth rates, on average, compared with non-reef-associated species (Extended Data Fig. 6). However, these accelerations in growth and reductions in size optima were not homogeneously distributed over time. Shifts towards a higher growth and lower size optima were concentrated in the Eocene (56–33.9 Ma). Thus, at the time of the highest recorded reef fish diversification in the Oligocene–Miocene (33.9–5.3 Ma)^{6,34}, most of the shifts in life history had already taken place millions of years before. Our results therefore call for a reinterpretation of the evolutionary events shaping one of the most diverse vertebrate radiations in the world.

Novelty in reef fish growth and size

Extant coral reef fish faunas are largely a product of key historical and evolutionary developments that took place throughout the Cenozoic Era. To characterize these developments, this Era was previously split into three major phases³⁵: the Palaeocene–Eocene (66–34 Ma), the Oligocene–Miocene (34–5.3 Ma) and the Pliocene–Pleistocene (5.3–0 Ma). The Palaeocene–Eocene was marked by the origins of most typical coral reef fish families (for example, Labridae, Apogonidae, Pomacentridae), whereas the Oligocene–Miocene was regarded as the

Article

most important time for reef fish functional differentiation, including the rise and expansion of small-bodied and fast-growing species⁶. Although the Miocene seems to have indeed been an important time for trophic innovations in reef fishes^{19,36,37}, our results suggest that this was not necessarily mirrored by growth and body size. Most evolutionary novelty in reef fish size and growth trajectories appears to have occurred at an earlier age, in the Eocene, which highlights this Epoch as a fundamental time for the evolution of fast-paced life histories. However, the Eocene shifts in growth evolutionary optima were not limited to small-bodied cryptobenthic species. These cryptobenthic lineages did indeed shift towards more extreme, high values of growth optima, but growth accelerations were widespread throughout the phylogeny (Fig. 2). This temporal congruence and phylogenetic spread in evolutionary regime shifts suggest that the Eocene might have been a time that indiscriminately favoured high growth rates across several reef fish lineages. This raises the question of what factors could have driven the accumulation of growth shifts in the Eocene.

Generally, the best predictors of patterns in individual growth for vertebrate populations are body size and temperature^{9,38}, underscored by the high relative importance of these factors in our predictive models (Supplementary Results). Maximum body length was indeed important for determining the magnitude of change in growth optima observed here (Fig. 2), with half of the shifts towards faster growth also happening towards smaller sizes (Extended Data Fig. 4). However, the Eocene shifts in growth rates occurred in lineages spanning a wide range of body sizes (for example, the goby *Eviota sigillata* has a maximum body length of 1.9 cm compared with the bream *Scolopsis margaritifera* with a maximum body length of 28 cm). It therefore seems probable that temperature had as strong influence as (or perhaps even stronger than) body size in the temporal accumulation of growth regime shifts in reef fishes. Indeed, the Eocene was the hottest Epoch of the Cenozoic⁵, with a climatic optimum that largely coincides with the highest density of positive growth and negative size shifts detected by our models (Fig. 1 and Extended Data Fig. 4). This suggests that the high temperatures of the Eocene might have provided the foundation for the evolution of faster life history strategies in reef fishes, which agrees with recent findings that fish develop smaller body sizes and faster growth in response to warming temperatures³⁹.

It is important to note that the frequency of shifts towards faster growth rates and smaller sizes was decoupled from the frequency of branching events in the reef fish phylogeny. We expected to find more shifts in growth trajectories happening in the Oligocene–Miocene, when most reef fish lineage diversification occurred^{6,19,34}, but this was not the case. This temporal decoupling strengthens the idea that there were specific abiotic and biotic conditions of the Eocene that underpinned the shifts in evolutionary regimes. It appears that high global temperatures may have driven the origins of fast-paced life histories in the Eocene, but it was not until the development of new coral reef habitat configurations in the Oligocene–Miocene⁶ that conditions favoured the expansion of reef fish lineages towards the fast end of life history strategies. In essence, the potential for fast life histories seems to have evolved well before the realized expansion of fast-growing and small-bodied reef fish lineages.

Conversely, the Eocene shifts in reef fish growth and size might have been the product of ecological release in the aftermath of the K/Pg mass extinction. For example, evidence from the fossil record suggest that niche expansion was facilitated by ecological opportunity in some fish lineages in the early Cenozoic^{40,41}. Thus, the rise of new life history strategies might represent a similar case. However, this scenario is less likely for two main reasons. First, evolutionary shifts are concentrated at around 20 million years after the K/Pg boundary and after the origin of most reef fish families, which is a substantial temporal latency for ecological novelty to arise; thus, fast life histories did not arise with the origin of most families, but several million years after. Second, under this latency scenario, one would expect shifts to be equally likely

towards both ends of the life history spectrum, but our results show that post-K/Pg regime shifts only occurred into faster growth optima. While asymmetric shifts are not per se evidence against this latency hypothesis, they cannot be explained by it, therefore requiring a third explanatory factor. Thus, these asymmetric shifts lower the parsimony of the latency hypothesis, further supporting the temperature hypothesis explained above. It appears that there were far fewer constraints into shifting towards accelerated life histories in the evolution of reef fishes than there were towards the slower end of the spectrum.

A new energetic regime on coral reefs

One of the most striking characteristics of present-day coral reefs is the diversity and numerical abundance of small-bodied fish species, particularly in the families Gobiidae, Blenniidae, Pomacentridae and Apogonidae⁶. Notably, all of these families belong to clades that have extreme values of growth evolutionary optima (Fig. 2), even when accounting for their average small body sizes (Fig. 3). However, there seems to be a disconnect between the timing of when these clades first shifted towards higher growth rate optima and when they became numerically abundant and diverse. In Gobiaria, for example, the regime shift in growth was estimated to occur in the Cretaceous (Fig. 2), at the origin of this clade; but only their molecular sequences can be traced this far back in time and there is little evidence in the fossil record to suggest that small-bodied gobiiform lineages were alive before the K/Pg boundary^{42,43}. Despite the uncertainty associated with the palaeontological record, fossils from the Early Cenozoic suggest that their abundance and diversity were not as high as they are in modern coral reefs^{6,44}. Thus, it appears that habitat shifts in the Miocene underpinned the success of an ancient fast-paced life history strategy that became increasingly advantageous with the formation of modern coral reef configurations.

Some species within the small-bodied, fast-growing fish families have strong associations with branching scleractinian corals in modern reefs⁴⁵. This raises the question of whether branching scleractinian corals could provide a clue to the Miocene diversification of fast life histories. Notably, the initial diversification of these coral growth forms coincides with the timing of expansion of small, fast-growing fish lineages. Modern scleractinian coral groups started to diversify in the Miocene^{18,46}, although the dominance of fast-growing branching forms, particularly in the family Acroporidae, is a product of a very recent expansion in the Pliocene–Pleistocene^{47,48}. Diversification patterns in fishes seem to be more associated with the Miocene expansion of coral growth forms than with the latter Pliocene–Pleistocene event. Thus, small-bodied, fast-growing fish lineages could have benefitted from the refuges provided by the structures of these early scleractinian corals. Indeed, to sustain increasingly fast growth, animals need to increase food intake, with frequent trade-offs between predation risk and foraging effort⁴. As a consequence, life in the fast lane can be evolutionarily advantageous only if lineages can somehow overcome the dangers of predation, while maintaining increased foraging rates as small-bodied organisms. Corals probably provided the necessary predation relief in the Miocene for many small-bodied, fast-growing fish lineages that originated earlier in the warm temperatures of the Eocene.

Today, some of the fastest-growing fish lineages appear to have taken a fundamental role in sustaining the productivity of coral reef fishes. Despite contributing relatively little to the process of biomass accumulation, cryptobenthic fishes are among the most important energetic currencies within modern coral reefs^{20,49}. Through extraordinary rates of mortality, very fast growth and likely enhanced larval retention, cryptobenthic reef fishes contribute between 20% and 70% of all consumed fish biomass on typical coral reefs around the world⁵⁰. The high-productivity high-mortality life history of cryptobenthic fishes is probably the end-product of a long evolutionary history, potentially shaped by thermally induced origins in the Eocene but sustained by subsequent key Miocene habitat changes and the expansion of modern reefs.

The initial shifts in life history evolutionary regimes reported here, and their subsequent expansion, therefore represent the foundations of the fast-turnover energetic dynamics that characterize the highly productive present-day coral reefs.

Conclusions

Here we show that the evolution of crucial life history traits, growth and size were highly skewed towards faster growth and smaller sizes in reef fishes. We posit that the high global temperatures of the Eocene may have favoured frequent and intense evolutionary shifts in reef fish life histories, while subsequent habitat changes in the Miocene may have provided the essential substrate for the survival and expansion of many small-bodied, fast-growing lineages. To our knowledge, this is the first documentation of large-scale, macroevolutionary patterns in growth rates for an entire vertebrate assemblage. As recently noted⁵¹, understanding size-related variation in life history traits during fish evolution is essential. Our research represents an important contribution in that direction, providing a roadmap for future studies to analyse macroevolutionary patterns in the life histories of other taxa.

Online content

Any methods, additional references, Nature Portfolio reporting summaries, source data, extended data, supplementary information, acknowledgements, peer review information; details of author contributions and competing interests; and statements of data and code availability are available at <https://doi.org/10.1038/s41586-023-06070-z>.

1. Wong, S., Bigman, J. S. & Dulvy, N. K. The metabolic pace of life histories across fishes. *Proc. R. Soc. B* **288**, 20210910 (2021).
2. Healy, K., Ezard, T. H. G., Jones, O. R., Salguero-Gómez, R. & Buckley, Y. M. Animal life history is shaped by the pace of life and the distribution of age-specific mortality and reproduction. *Nat. Ecol. Evol.* **3**, 1217–1224 (2019).
3. Charnov, E. L. & Berrigan, D. Evolution of life history parameters in animals with indeterminate growth, particularly fish. *Evol. Ecol.* **5**, 63–68 (1991).
4. Dmitriew, C. M. The evolution of growth trajectories: what limits growth rate? *Biol. Rev.* **86**, 97–116 (2011).
5. Westerhold, T. et al. An astronomically dated record of Earth's climate and its predictability over the last 66 million years. *Science* **369**, 1383–1387 (2020).
6. Bellwood, D. R., Goatley, C. H. R. & Bellwood, O. The evolution of fishes and corals on reefs: form, function and interdependence. *Biol. Rev.* **92**, 878–901 (2017).
7. Stearns, S. C. Trade-offs in life-history evolution. *Funct. Ecol.* **3**, 259–268 (1989).
8. Ricklefs, R. E. & Wikelski, M. The physiology/life-history nexus. *Trends Ecol. Evol.* **17**, 462–468 (2002).
9. Brown, J. H., Gillooly, J. F., Allen, A. P., Savage, V. M. & West, G. B. Toward a metabolic theory of ecology. *Ecology* **85**, 1771–1789 (2004).
10. Jennings, S., Greenstreet, S. P. R. & Reynolds, J. D. Structural change in an exploited fish community: a consequence of differential fishing effects on species with contrasting life histories. *J. Anim. Ecol.* **68**, 617–627 (1999).
11. Reynolds, J. D. In *Macroecology* (eds Blackburn, T. M. & Gaston, K. J.) 195–217 (Blackwell Publishing, 2003).
12. Thygesen, U. H., Farnsworth, K. D., Andersen, K. H. & Beyer, J. E. How optimal life history changes with the community size-spectrum. *Proc. R. Soc. B* **272**, 1323–1331 (2005).
13. Arendt, J. D. Adaptive intrinsic growth rates: an integration across taxa. *Q. Rev. Biol.* **72**, 149–177 (1997).
14. Heino, M. & Kaitala, V. Evolution of resource allocation between growth and reproduction in animals with indeterminate growth. *J. Evol. Biol.* **12**, 423–429 (1999).
15. Caley, M. J. & Schwarzkopf, L. Complex growth rate evolution in a latitudinally widespread species. *Evolution* **58**, 862–869 (2004).
16. Lindgren, B. & Laurila, A. Proximate causes of adaptive growth rates: growth efficiency variation among latitudinal populations of *Rana temporaria*. *J. Evol. Biol.* **18**, 820–828 (2005).
17. Abrams, P. A., Leimar, O., Nylin, S. & Wiklund, C. The effect of flexible growth rates on optimal sizes and development times in a seasonal environment. *Am. Nat.* **147**, 381–395 (1996).
18. Santodomingo, N., Wallace, C. C. & Johnson, K. G. Fossils reveal a high diversity of the staghorn coral genera *Acropora* and *Isopora* (Scleractinia: Acroporidae) in the Neogene of Indonesia. *Zool. J. Linn. Soc.* **175**, 677–763 (2015).
19. Siqueira, A. C., Morais, R. A., Bellwood, D. R. & Cowman, P. F. Trophic innovations fuel reef fish diversification. *Nat. Commun.* **11**, 2669 (2020).
20. Brandl, S. J. et al. Demographic dynamics of the smallest marine vertebrates fuel coral reef ecosystem functioning. *Science* **364**, 1189–1192 (2019).
21. Morais, R. A., Siqueira, A. C., Smallhorn-West, P. F. & Bellwood, D. R. Spatial subsidies drive sweet spots of tropical marine biomass production. *PLoS Biol.* **19**, e3001435 (2021).
22. Frýdllová, P. et al. Determinate growth is predominant and likely ancestral in squamate reptiles. *Proc. R. Soc. B* **287**, 20202737 (2020).
23. Bellwood, D. R. & Wainwright, P. C. In *Coral Reef Fishes: Dynamics and Diversity on a Complex Ecosystem* (ed. Sale, P. F.) 5–32 (Academic, 2002).
24. Depczynski, M. & Bellwood, D. R. Extremes, plasticity, and invariance in vertebrate life history traits: insights from coral reef fishes. *Ecology* **87**, 3119–3127 (2006).
25. Morais, R. A. & Bellwood, D. R. Pelagic subsidies underpin fish productivity on a degraded coral reef. *Curr. Biol.* **29**, 1521–1527 (2019).
26. Morais, R. A. & Bellwood, D. R. Global drivers of reef fish growth. *Fish Fish.* **19**, 874–889 (2018).
27. Beukhof, E. et al. Marine fish traits follow fast-slow continuum across oceans. *Sci. Rep.* **9**, 17878 (2019).
28. Denney, N. H., Jennings, S. & Reynolds, J. D. Life-history correlates of maximum population growth rates in marine fishes. *Proc. R. Soc. Lond. B* **269**, 2229–2237 (2002).
29. Morais, R. A. & Bellwood, D. R. Principles for estimating fish productivity on coral reefs. *Coral Reefs* **39**, 1221–1231 (2020).
30. Rabosky, D. L. et al. An inverse latitudinal gradient in speciation rate for marine fishes. *Nature* **559**, 392–395 (2018).
31. Uyeda, J. C. & Harmon, L. J. A novel Bayesian method for inferring and interpreting the dynamics of adaptive landscapes from phylogenetic comparative data. *Syst. Biol.* **63**, 902–918 (2014).
32. Ghezelayagh, A. et al. Prolonged morphological expansion of spiny-rayed fishes following the end-Cretaceous. *Nat. Ecol. Evol.* **6**, 1211–1220 (2022).
33. Mitov, V., Bartoszek, K. & Stadler, T. Automatic generation of evolutionary hypotheses using mixed Gaussian phylogenetic models. *Proc. Natl Acad. Sci. USA* **116**, 16921–16926 (2019).
34. Cowman, P. F. & Bellwood, D. R. Coral reefs as drivers of cladogenesis: expanding coral reefs, cryptic extinction events, and the development of biodiversity hotspots. *J. Evol. Biol.* **24**, 2543–2562 (2011).
35. Bellwood, D. R., Goatley, C. H. R., Cowman, P. F., Bellwood, O. & Mora, C. In *Ecology of Fishes on Coral Reefs* (ed. Mora, C.) 55–63 (Cambridge Univ. Press, 2015).
36. Cowman, P. F., Bellwood, D. R. & van Herwerden, L. Dating the evolutionary origins of wrasse lineages (Labridae) and the rise of trophic novelty on coral reefs. *Mol. Phylogenet. Evol.* **52**, 621–631 (2009).
37. Bellwood, D. R., Hoey, A. S., Bellwood, O. & Goatley, C. H. R. Evolution of long-toothed fishes and the changing nature of fish-benthos interactions on coral reefs. *Nat. Commun.* **5**, 3144 (2014).
38. Gillooly, J. F., Charnov, E. L., West, G. B., Savage, V. M. & Brown, J. H. Effects of size and temperature on developmental time. *Nature* **417**, 70–73 (2002).
39. Lindmark, M., Audzinyte, A., Blanchard, J. L. & Gårdmark, A. Temperature impacts on fish physiology and resource abundance lead to faster growth but smaller fish sizes and yields under warming. *Glob. Change Biol.* **28**, 6239–6253 (2022).
40. Friedman, M. Explosive morphological diversification of spiny-finned teleost fishes in the aftermath of the end-Cretaceous extinction. *Proc. R. Soc. B* **277**, 1675–1683 (2010).
41. Sibert, E. C. & Norris, R. D. New age of fishes initiated by the Cretaceous–Paleogene mass extinction. *Proc. Natl Acad. Sci. USA* **112**, 8537–8542 (2015).
42. Patterson, C. An overview of the early fossil record of acanthomorphs. *Bull. Mar. Sci.* **52**, 29–59 (1993).
43. Marrama, G., Giusberti, L. & Carnevale, G. A Rupelian coral reef fish assemblage from the Venetian Southern Alps (Bericì Hills, NE Italy). *Riv. Ital. Paleontol. S.* **128**, 469–513 (2022).
44. Marrama, G., Garbelli, C. & Carnevale, G. A clade-level morphospace for the Eocene fishes of Bolca: patterns and relationships with modern tropical shallow marine assemblages. *B. Soc. Paleontol. Ital.* **55**, 139–156 (2016).
45. Coker, D. J., Wilson, S. K. & Pratchett, M. S. Importance of live coral habitat for reef fishes. *Rev. Fish Biol. Fish.* **24**, 89–126 (2014).
46. Mihaljević, M., Renema, W., Welsh, K. & Pandolfi, J. M. Eocene–Miocene shallow-water carbonate platforms and increased habitat diversity in Sarawak, Malaysia. *Palaios* **29**, 378–391 (2014).
47. Renema, W. et al. Are coral reefs victims of their own past success? *Sci. Adv.* **2**, e150085 (2016).
48. Siqueira, A. C., Kiessling, W. & Bellwood, D. R. Fast-growing species shape the evolution of reef corals. *Nat. Commun.* **13**, 2426 (2022).
49. Depczynski, M., Fulton, C. J., Marnane, M. J. & Bellwood, D. R. Life history patterns shape energy allocation among fishes on coral reefs. *Oecologia* **153**, 111–120 (2007).
50. Brandl, S. J. et al. Response to Comment on “Demographic dynamics of the smallest marine vertebrates fuel coral reef ecosystem functioning”. *Science* **366**, eaaz1301 (2019).
51. Choat, J. H. Marine biology: ageing a ‘living fossil’. *Curr. Biol.* **31**, R998–R1000 (2021).
52. Schietekatte, N. M. D., Brandl, S. J. & Casey, J. M. fishualize: color palettes based on fish species. R package version 0.2.0 (2020).

Publisher's note Springer Nature remains neutral with regard to jurisdictional claims in published maps and institutional affiliations.

Springer Nature or its licensor (e.g. a society or other partner) holds exclusive rights to this article under a publishing agreement with the author(s) or other rightsholder(s); author self-archiving of the accepted manuscript version of this article is solely governed by the terms of such publishing agreement and applicable law.

© The Author(s), under exclusive licence to Springer Nature Limited 2023

Methods

Foundations of fish growth

To calculate the growth in coral reef fishes, we adopted a framework developed previously²⁶, standardizing parameters derived from the von Bertalanffy Growth Model (VBGM)⁵³. The VBGM has been applied to thousands of fish species and has been used in both ecology- and fisheries-related studies to model the ontogenetic growth of fishes. In brief, the VBGM reflects a balance between the two metabolic processes affecting growth: anabolism, the production of body materials, and catabolism, the consumption of body materials. By integrating both anabolic and catabolic processes into the VBGM, we can derive the growth parameters L_{∞} , which reflects the average asymptotic size of the population, and the von Bertalanffy growth coefficient K (year⁻¹), which is indicative of the mean rate at which the population approaches the population asymptotic size (L_{∞}). Both L_{∞} and K are sensitive to the methodology used and can have different interpretations at the individual or population level, which can be problematic for cross-scale studies²⁶. To circumvent these issues, we standardized K to the maximum body size (that is, length) recorded for each species to generate theoretical projections of fish growth that are comparable across species. This process then generates a composite, standardized life history trait, which encapsulates the trade-off between maximum size and growth. Following ref. 26, we also directly considered the ageing method used to collect the size-at-age data fitted by the VBGM in each case as a variable in our predictive model (see below).

Collating a dataset of reef fish growth

We first conducted a systematic review of the recent, published literature (from 2019 to June 2021) on coral reef fish growth to build on the dataset created previously²⁶. Our search mirrored the same criteria as used previously²⁶, including 49 different families, 46 of which were previously listed as reef fishes²³. For each species, we recorded the maximum length, the method by which length was measured (that is, total length (TL), standard length (SL) or fork length (FL)), the ageing method, the von Bertalanffy growth parameters L_{∞} and K and, when available, the length-weight conversion factors a and b . We converted all estimates of maximum size and L_{∞} to TL using the length-length conversion factors from FishBase⁵⁴. Using the same quality checks as performed previously²⁶ (Supplementary Methods), we added an additional 58 growth curves to the dataset for a total of 1,979 growth curves, belonging to 596 species.

We used collated values of L_{∞} and K to calculate standardized, theoretical projections of growth for each species (compare with ref. 26). We calculated K_{\max} (unit year⁻¹) as the rate that fishes would reach their asymptotic size L_{∞} if they grew to the maximum reported size for that species (L_{\max} ; see ref. 26 and the Supplementary Methods for equations). This metric can therefore be intuitively thought of as the number of maximum body lengths attainable through growth in a year. In contrast to the growth performance index (\emptyset)^{26,55}, which offers a similar standardization solution, K_{\max} is readily interpretable biologically, and will therefore be the focus of this study. We used the same procedures to model K_{\max} as a function of environmental and ecological variables as used previously²⁶, which included georeferencing the growth curve and extracting mean sea surface temperature for each new record and classifying each new recorded species according to their diet and relationship to the reef. We also recorded the ageing methods used to obtain the size-at-age data used to fit the VBGM in each study. The detailed procedures used to assert geographical coordinates and extract temperature data, as well as the exact definitions of each categorical variable, were described previously²⁶.

Predicting reef fish growth

We used temperature, maximum size, diet, position and method in an extreme gradient boosted regression tree (BRT) to predict K_{\max} for

all the species in a published molecular phylogeny³⁰ for which there are no empirically measured growth data. Data from these predictors were obtained from ref. 26, and were originally sourced from literature sources and FishBase⁵⁴. BRTs are a form of machine learning that combines multiple decision trees with a boosting algorithm and can achieve a high predictive accuracy⁵⁶. In contrast to other statistical models, BRTs are not restricted by nonlinear relationships, complex interactions or missing data and can handle collinear variables⁵⁶. We used the XGBoost (v.1.4.1.1) package⁵⁷ in R (v.4.1.0) owing to its superior performance in controlling for overfitting and faster speed compared to other packages^{57,58}.

Using a Gamma distribution to model K_{\max} , we selected hyperparameters mirroring the two-step tuning method done previously²⁶. We first selected hyperparameters by varying the learning rate (eta), the regularizing parameter gamma, the maximum tree depth and the subsample rate by choosing the combination of values that minimized the negative log likelihood. We then varied the values from the first step by drawing values from a normal distribution, truncated to $\pm 10\%$ of each hyperparameter value. Using this two-step approach, we were able to reduce the negative log likelihood from 2.0 to 1.77 using the following hyperparameter values: eta = 0.19, gamma = 0.46, maximum tree depth = 5 and subsample rate = 0.75.

To model and predict K_{\max} , we used a cross-validation approach by building the model on a training set (80% of the data) and assessing the model's performance on the remaining test set (20%). We assessed model performance by measuring the average bias of the model by subtracting the predicted K_{\max} values from the observed in the test set, whereby a well-fitted model should have a bias close to zero. We also measured model performance by fitting a linear model through the log-log-transformed predicted-observed K_{\max} values and extracted the corresponding r^2 . Finally, we used the model to predict the K_{\max} values for fishes that were found in the phylogeny but were missing empirically measured von Bertalanffy growth parameters. Overall, empirical and estimated values were evenly distributed across taxonomic groups (Supplementary Fig. 1a), body sizes (Supplementary Fig. 1b) and temperatures (Supplementary Fig. 1c). Owing to the stochastic model-building process of BRTs, we bootstrapped each iteration 1,000 times and used the mean predicted K_{\max} value across all iterations. Model diagnostics and partial dependence plots are shown in Supplementary Figs. 2 and 3, respectively.

Evolutionary regimes of reef fish growth

From the total of 596 species with empirical growth data, 525 were present in the phylogenetic tree of ref. 30. Another 1,949 species from the selected reef-associated fish families were also present in the tree but had no associated growth data. After adding the K_{\max} values predicted by the BRTs for these species, we ended up with a dataset containing 2,474 species for which we had both phylogenetic and growth data (empirical and predicted). We only used the time-calibrated phylogeny of ref. 30 that was built using genetic data in the main results to minimize issues with topological uncertainty in the ancestral state reconstructions. However, we repeated the analyses using the backbone (see details below) of the most recent phylogenomic tree of spiny-rayed fishes³² (findings presented in the Extended Data Fig. 3). Our first goal with the phylogenetic reconstructions was to detect the location, timing, number and magnitude of shifts in the adaptive optima of K_{\max} values along the reef fish phylogenetic tree. To that end, we used the bayou R package (v.2.2.0)³¹ to fit multi-optima Ornstein–Uhlenbeck (OU) models of continuous trait evolution. This package uses a Bayesian reversible-jump method to identify significant shifts in the evolutionary regime of a continuously distributed trait, without the need to specify any a priori hypotheses about the location of these shifts in the phylogeny³¹. The main parameters estimated for the OU regime describe the rate of adaptation (α), the magnitude of uncorrelated diffusion per unit of time (σ^2) and the optimum trait value (θ) associated

with each regime shift³¹. For our models, we set half-Cauchy priors for α and σ^2 , and a normal prior for θ (with mean and s.d. defined by the full dataset of K_{\max} values). Moreover, we assigned a conditional Poisson prior for the number of shifts, with the maximum number of possible regime shifts equal to half the number of tips in the phylogeny. We also used the average bias estimated by the BRTs as an indication of the potential measurement error associated with K_{\max} values in the models. Finally, we set a maximum of one shift allowed per branch, and equal probability of shifts across all branches in the tree. We ran two independent Markov Chain Monte Carlo (MCMC) chains, each with a random starting point, to assess whether models were converging towards similar solutions. Each chain was run for ten million generations, sampling parameters every 1,000 generations. Convergence was evaluated through the effective sample sizes of all parameters, after discarding the first 30% samples of each chain as burn-in. All K_{\max} values were \log_{10} -transformed before the analyses to reduce the extreme skew towards low growth values.

We combined the results from both MCMC chains to assess the locations of the most likely shifts in the evolutionary optima of K_{\max} . Only shifts detected with 75% posterior probability were considered in our main results. Typically, studies applying this model use a lower threshold for the detection of shifts, around 30% posterior probability, which already represents 30 times the set prior probability. However, we used the conservative approach of 75% to reduce the chance of finding spurious regime shifts given the large size of our phylogenetic tree. Using an extremely conservative posterior probability of 90% reduces the number of shifts detected but does not change our overall temporal patterns (Supplementary Fig. 4). We also excluded three branches that passed the posterior probability criteria, but had three or fewer descendant species, which can also produce spurious regime shifts. Although the MCMC chains were very consistent in identifying which branches had regime shifts in the evolutionary optima of K_{\max} , the precise location of the shift along the branch is hard to estimate. Thus, to standardize across regime shifts, here we report shift locations as the nodes representing the most recent common ancestor of all descendants of the branch identified by the model. In other words, we consider specific locations as the crown age of regime shifts. After detecting these shifts, we calculated their probabilities after accounting for the range of possible locations where they could occur along the tree at each geological epoch. We did this by dividing the sum of shifts found per epoch by the total branch length in the same time period, calculated using the phytools R package (v.1.0.3)⁵⁹.

After applying the necessary filters to the multi-optima OU model derived from bayou, we compared it against a single evolutionary optimum (single-optimum OU) model or a Brownian motion model to assess whether these simpler models might represent a better fit to our data. This analysis was performed using the mvMORPH R package (v.1.1.4)⁶⁰, which requires an a priori definition of regime shift locations in multi-optima OU models. We therefore used the shifts detected through bayou in the maximum likelihood framework of mvMORPH to perform our model comparison. The multi-optima OU model was detected as having a far better fit when compared to the single-optimum OU and the Brownian motion models ($\Delta AICc > 20$; Supplementary Table 1).

We followed the exact same modelling procedures described above to run the bayou model with species maximum body length (body size) as input instead of the growth coefficient. This was done to assess whether the results found for growth would be similar to the ones found for body size (Extended Data Fig. 4). Importantly, our intention here was not to tease apart the effects of growth independent of body size, given how strongly correlated these traits are. Moreover, we assessed the sensitivity of our growth results against an alternative dating scheme based on a recent phylogenomic analysis³². This tree was inferred using ultraconserved elements and sampled the majority of spiny-rayed fish families, including the ones analysed here. However, it had a substantially lower

species level sampling when compared with ref. 30. Thus, to be able to have the same dense sampling as the latter, we used the congruification⁶¹ approach, as implemented in the geiger R package (v.2.0.9)⁶². This method uses a reference phylogeny to time-calibrate a target tree based on shared nodes of higher taxa. We therefore selected all nodes that were concordant between the ref. 30 and the ref. 32 trees at the genus level to generate our reference chronogram. We then applied the method of congruification to include all of the tips from the target tree³⁰ and generate an input with time calibration points for subsequent use in treePL⁶³. Through this algorithm, we finally estimated divergence times in the target tree on the basis of the reference calibration points from ref. 32, using its penalized likelihood approach. Importantly, although we followed the best practices for this type of analysis (that is, performing priming to select the best optimization parameters and selecting the best smoothing value from a cross-validation analysis)⁶³, the calibration scheme generated divergence times that are at odds with the fossil record. For example, the origin of Apogonidae in the new chronogram is estimated at around 43 Ma; however, there are fossil apogonids described from about 50 Ma (ref. 64). The family Chaetodontidae has its crown estimated at about 17 Ma, while the oldest fossil within this family is approximately 33 Ma⁴³. The crown Pomacentridae gets dated at about 28 Ma, which is far from the oldest described fossil from the Palaeocene or from multiple examples from the Eocene⁶⁵. Owing to these inconsistencies, we kept the phylogeny of ref. 30 as our main chronogram of analysis and we used the sensitivity analysis described here as a likely representation of the youngest possible limit of uncertainty around the estimated timing of shifts in our main results.

Evolution of allometry (growth and size)

As expected by theoretical models⁹, the growth coefficient K_{\max} is strongly correlated with species maximum body size in reef fishes²⁶. We were therefore also interested in assessing whether there is any evidence of shifts in the evolutionary regime of the allometric relationship between these two variables. We approached this question by applying the recently developed mixed Gaussian phylogenetic model (MGPM)³³. This model accounts for the heterogeneity of the evolutionary processes operating in different parts of the tree and jointly infers different types of Gaussian models (that is, Brownian motion and OU) to each of the distinct evolutionary regimes detected³³. The MGPM represents a state-of-the-art phylogenetic model of trait evolution and was specifically designed to detect changes in evolutionary regimes of allometric relationships³³. However, given its computational complexity, it is difficult to achieve convergence for this model when using large phylogenetic trees, such as the one used here.

To be able to run the MGPM with our dataset, we first pruned our reef fish tree to the genus level, which resulted in a phylogeny containing 602 tips. We then summarized both maximum body length and K_{\max} as the \log_{10} -transformed values at the most recent common ancestor node of each genus, calculated through ancestral state reconstructions. These reconstructions were performed using the 'fastAnc' function from phytools. For monotypic genera we used the trait values from the only species within each genus. We then used the PCMBBase (v.1.2.12) and PCMFit (v.1.1.0) libraries in R^{33,66} to fit the six default models of allometric trait evolution to our data. These models were described previously³³. In brief, they include combinations of global Brownian motion and OU models in which traits are either uncorrelated or correlated in different ways (Supplementary Table 2). After fitting these six models, we fit the MGPM model, which was built to detect nodes along the tree with shifts in the evolutionary regime of the allometric relationship between maximum body size and K_{\max} . Finally, we performed model comparisons, which demonstrated strong support for the MGPM when compared to the six default models ($\Delta AICc > 20$; Supplementary Table 2). After finding the MGPM as the best-fit evolutionary model for the relationship between maximum body length and K_{\max} in reef fishes, we assessed the location of regime shifts along the phylogenetic tree

Article

(Extended Data Fig. 5). Each shift is associated with a specific Gaussian process, from which we extracted the respective slopes and the intercepts for the allometric relationship from the MGPM model output.

Reporting summary

Further information on research design is available in the Nature Portfolio Reporting Summary linked to this article.

Data availability

The datasets generated and/or analysed as part of this study are available at Zenodo (<https://doi.org/10.5281/zenodo.7797270>)⁶⁷. There are no restrictions on data availability. The phylogeny used in the main analyses was downloaded from The Fish Tree of Life (<https://fishtreeoflife.org>). Publicly available datasets used in the study include: FishBase (<http://www.fishbase.org>) and the data repository of ref. 26 (<https://doi.org/10.4225/28/5ae8f3cc790f9>). Source data are provided with this paper.

Code availability

The R (v.4.1.0) packages used were as follows: tidyverse, ggplot2, ape, phytools, geiger, ggtree, cowplot, viridis, raster, parallel, XGBoost, Matrix, pdp, data.table, png, grid, phangorn, bayou, mvMORPH, PCMBase, PCMBaseCpp and PCMFit. Package versions are provided in the Reporting Summary. The codes used during this study are available at Zenodo (<https://doi.org/10.5281/zenodo.7797270>)⁶⁷.

53. von Bertalanffy, L. Problems of organic growth. *Nature* **163**, 156–158 (1949).
54. Froese, R. & Pauly, D. FishBase. Version 04/2021 (2021); www.fishbase.org.
55. Pauly, D. Gill size and temperature as governing factors in fish growth: a generalization of von Bertalanffy's growth formula. *Ber. Inst. Meeresk. Kiel* **63**, 1–156 (1979).
56. Elith, J., Leathwick, J. R. & Hastie, T. A working guide to boosted regression trees. *J. Anim. Ecol.* **77**, 802–813 (2008).
57. Chen, T. & Guestrin, C. XGBoost: a scalable tree boosting system. In Proc. 22nd ACM SIGKDD International Conference on Knowledge Discovery and Data Mining 785–794 (ACM, 2016).
58. Mitchell, R. & Frank, E. Accelerating the XGBoost algorithm using GPU computing. *PeerJ Comput. Sci.* **3**, e127 (2017).
59. Revell, L. J. Phytools: an R package for phylogenetic comparative biology (and other things). *Methods Ecol. Evol.* **3**, 217–223 (2012).
60. Clavel, J., Escarguel, G. & Merceron, G. mvMORPH: an R package for fitting multivariate evolutionary models to morphometric data. *Methods Ecol. Evol.* **6**, 1311–1319 (2015).
61. Eastman, J. M., Harmon, L. J. & Tank, D. C. Congruification: support for time scaling large phylogenetic trees. *Methods Ecol. Evol.* **4**, 688–691 (2013).
62. Harmon, L. J., Weir, J. T., Brock, C. D., Glor, R. E. & Challenger, W. GEIGER: investigating evolutionary radiations. *Bioinformatics* **24**, 129–131 (2008).
63. Smith, S. A. & O'Meara, B. C. TreePL: divergence time estimation using penalized likelihood for large phylogenies. *Bioinformatics* **28**, 2689–2690 (2012).
64. Bannikov, A. F. Revision of some Eocene fishes from Bolca, Northern Italy, previously classified with the Apogonidae and Enoplosidae. *Stud. Ric. Giacimenti Terziari Bolca* **12**, 65–76 (2008).
65. Cantalice, K. M., Alvarado-Ortega, J., Bellwood, D. R. & Siqueira, A. C. Rising from the ashes: the biogeographic origins of modern coral reef fishes. *Bioscience* **72**, 769–777 (2022).
66. Mitov, V., Bartoszek, K., Asimomitis, G. & Stadler, T. Fast likelihood calculation for multivariate Gaussian phylogenetic models with shifts. *Theor. Popul. Biol.* **131**, 66–78 (2020).
67. Siqueira, A. C., Yan, H. F., Morais, R. A. & Bellwood, D. R. Data from “The evolution of fast-growing coral reef fishes”. Zenodo <https://doi.org/10.5281/zenodo.7797270> (2023).

Acknowledgements We thank J. Uyeda and V. Mitov for assistance with their R packages. Funding was provided by the Australian Research Council (D.R.B., LF190100062), with a Postdoctoral Fellowship to A.C.S. and a PhD Scholarship to H.F.Y. Funding for H.F.Y. was also provided by a Natural Sciences and Engineering Research Council of Canada Postgraduate Doctoral Scholarship. R.A.M. is supported by a Branco Weiss Fellowship Society in Science and a PSL Junior Fellowship.

Author contributions A.C.S., H.F.Y., R.A.M. and D.R.B. conceived the study. A.C.S., H.F.Y. and R.A.M. collected the data. A.C.S. and H.F.Y. performed the analyses and wrote the first draft of the manuscript. R.A.M. and D.R.B. contributed substantially to revisions.

Competing interests The authors declare no competing interests.

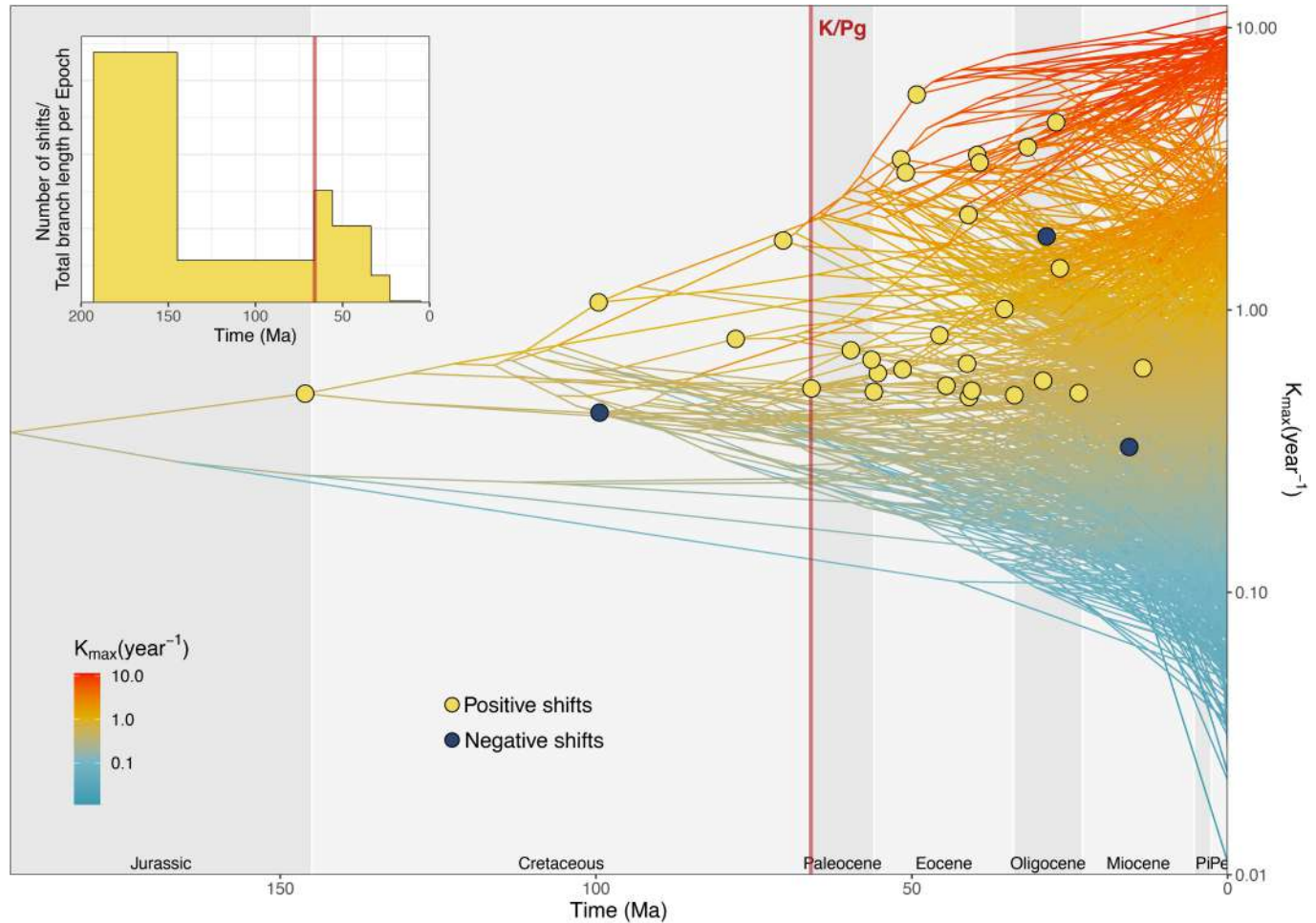
Additional information

Supplementary information The online version contains supplementary material available at <https://doi.org/10.1038/s41586-023-06070-z>.

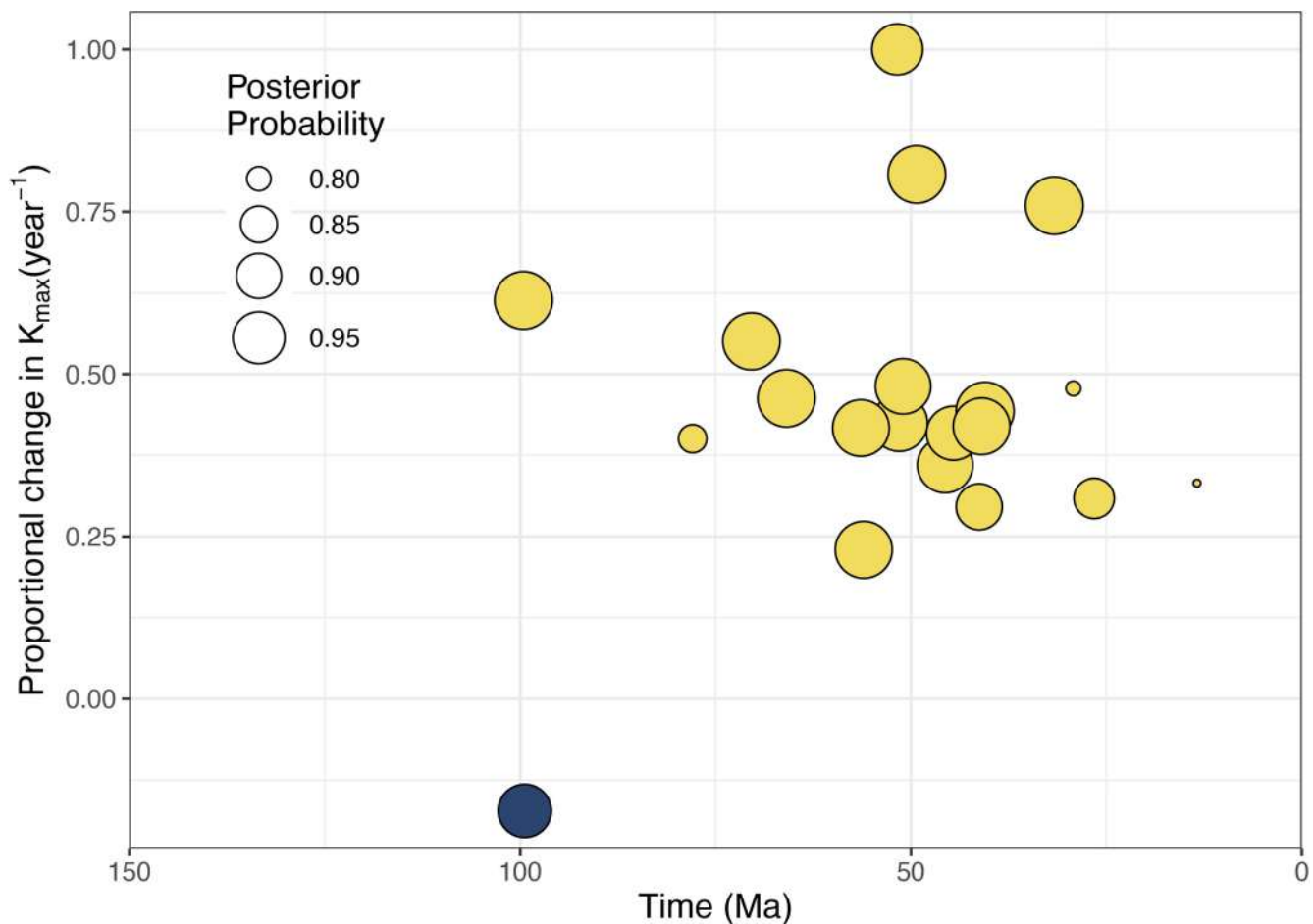
Correspondence and requests for materials should be addressed to Alexandre C. Siqueira.

Peer review information *Nature* thanks Tim Coulson, Luiz Rocha and the other, anonymous, reviewer(s) for their contribution to this work. Peer reviewer reports are available.

Reprints and permissions information is available at <http://www.nature.com/reprints>.

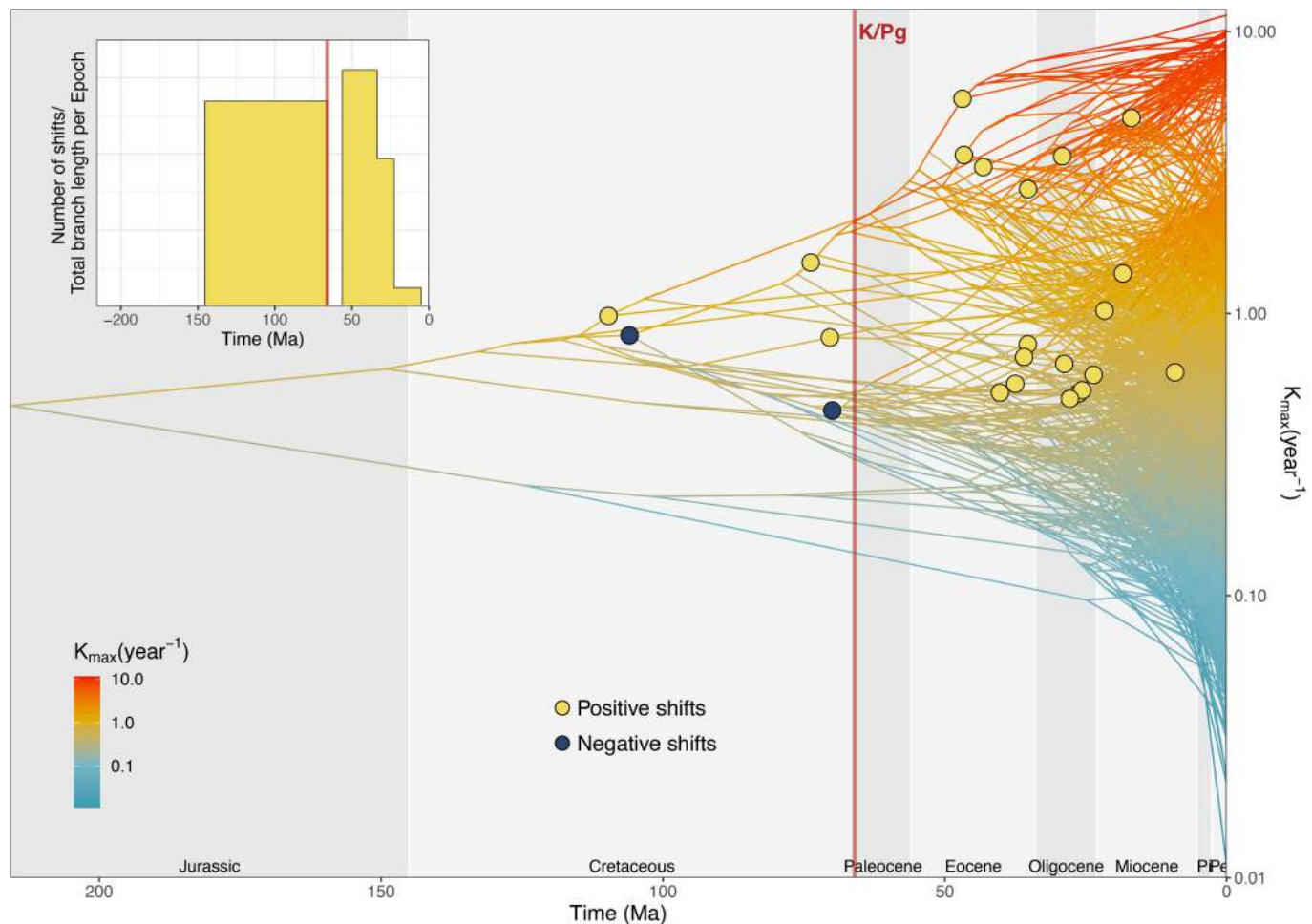


depicts the number of positive shifts divided by the total branch length in the phylogeny per geological epoch (y-axis) through time (x-axis). This metric gives an indication of the probability of shifts controlled by the availability of locations for them to occur, which is biased towards very old shifts. We note that the higher number of shifts/branch length detected for the Jurassic is a product of this bias and should be interpreted with caution given that it is the result of only one shift in that Period. The red line represents the Cretaceous-Paleogene (K/Pg) boundary. Pi: Pliocene; Pe: Pleistocene.



Extended Data Fig. 2 | Proportional change in reeffish K_{max} evolutionary optima through time. Light-yellow points represent shifts toward higher values of evolutionary optima (i.e. faster growth rates), while the dark-blue

point represents the opposite. The size of points is scaled according to their posterior probability in Ornstein–Uhlenbeck models.

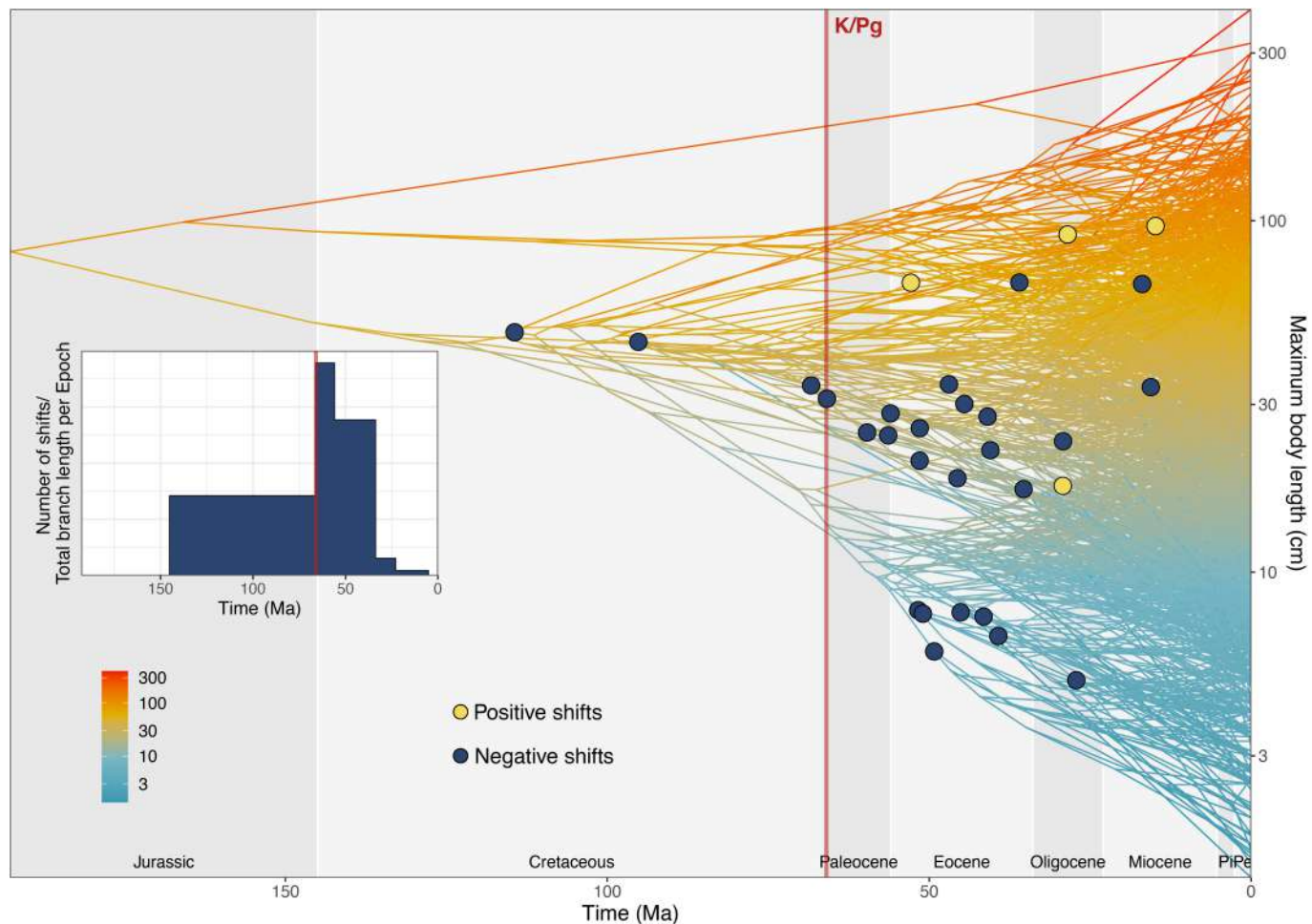


Extended Data Fig. 3 | Phylogenetic reconstruction of reeffish growth.

Standardized growth coefficient (K_{max}) reconstructed through time across the phylogenetic tree of coral reef-associated fishes, recalibrated based on Ghezelayagh *et al.*³² (see Methods). The points represent estimated shifts in the evolutionary regime of growth detected through multi-optima Ornstein–Uhlenbeck models. Light-yellow points represent shifts toward higher values of evolutionary optima (i.e. faster growth rates), while dark-blue points

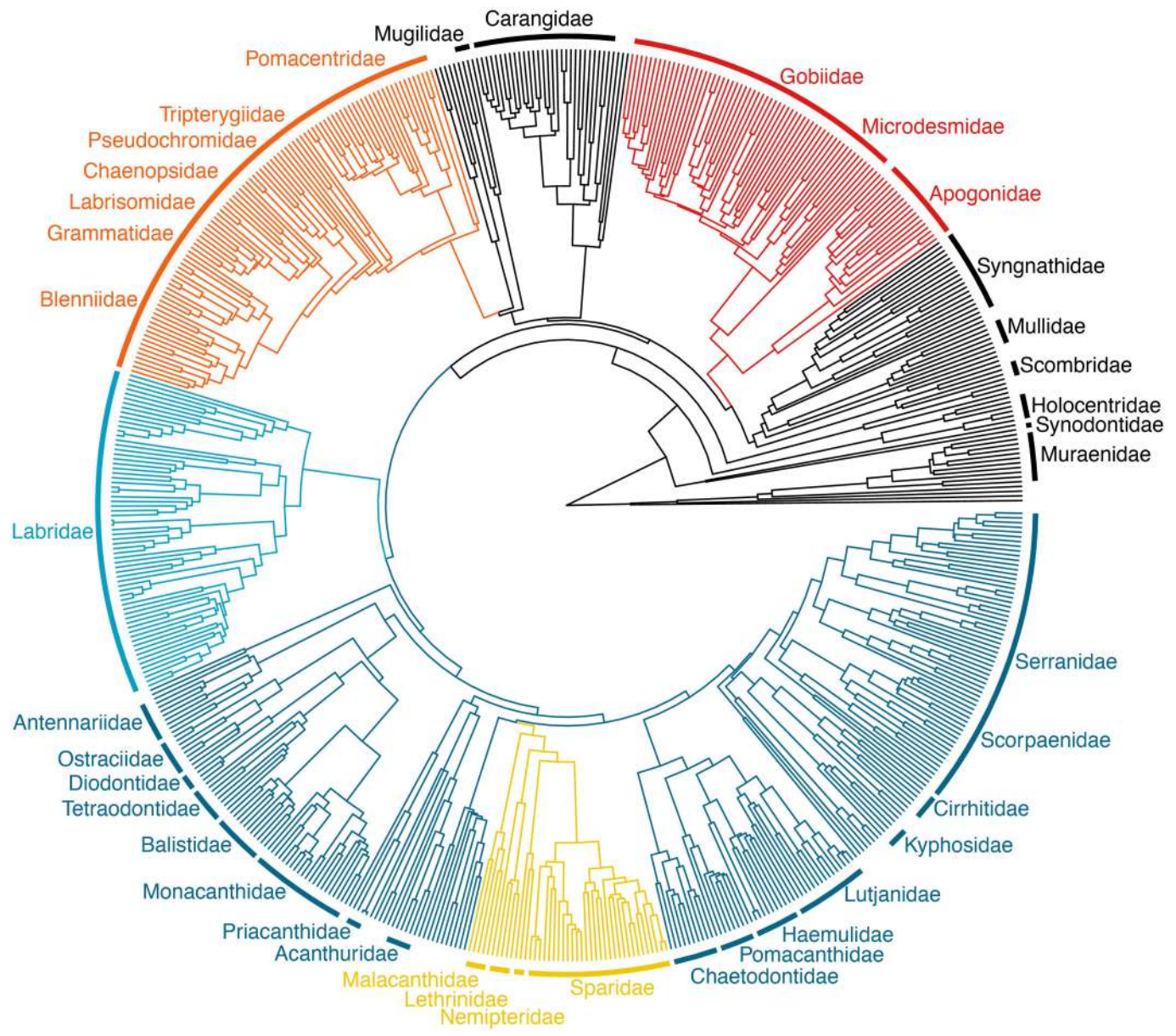
represent the opposite. Please note that the y-axis is on a \log_{10} scale. The inset depicts the number of positive shifts divided by the total branch length in the phylogeny per geological epoch (y-axis) through time (x-axis). This metric gives an indication of the probability of shifts controlled by the availability of locations for them to occur. The red line represents the Cretaceous–Paleogene (K/Pg) boundary. Pi: Pliocene; Pe: Pleistocene.

Article



Extended Data Fig. 4 | Phylogenetic reconstruction of reef fish body size. Maximum body length reconstructed through time across the phylogenetic tree of coral reef-associated fishes. The points represent estimated shifts in the evolutionary regime of body size detected through multi-optima Ornstein–Uhlenbeck models. Light-yellow points represent shifts toward higher values of evolutionary optima (i.e. larger body sizes), while dark-blue points represent

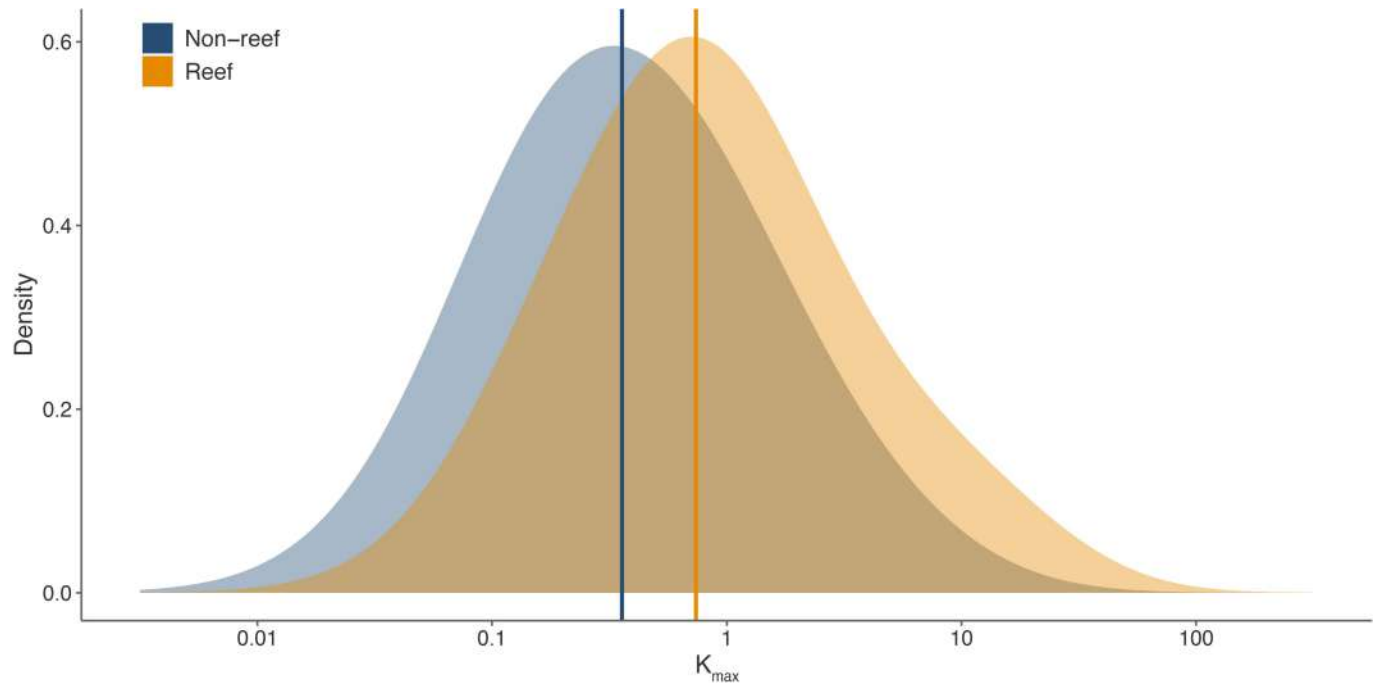
the opposite. Please note that the y-axis is on a \log_{10} scale. The inset depicts the number of negative shifts (i.e. towards smaller body sizes) divided by the total branch length in the phylogeny per geological epoch (y-axis) through time (x-axis). This metric gives an indication of the probability of shifts controlled by the availability of locations for them to occur. The red line represents the Cretaceous-Paleogene (K/Pg) boundary. Pi: Pliocene; Pe: Pleistocene.



Extended Data Fig. 5 | Evolutionary regimes in the allometry growth/body size in reef fishes. Reef fish phylogeny at the genus level with depicted evolutionary regimes for the allometric relationship between the growth coefficient (K_{max}) and maximum body length. The different colours across the branches represent the clades with different evolutionary regimes detected

by the mixed Gaussian phylogenetic model (see Methods). The coefficients estimated for each regime are shown in Fig. 3, with the respective colours. External arcs show the extant families represented by each clade, along with respective allometric evolutionary regime.

Article



Extended Data Fig. 6 | Empirical K_{max} values for reef vs. non-reef fish species.

Density plots illustrating the distribution of empirical K_{max} values for coral reef-associated species considered in this study (orange) and non-reef-

associated species (blue). Details on data collection for non-reef-associated species can be found in the supplementary material. The thick lines indicate the median K_{max} values for each group. Please note that the x-axis is on a log₁₀ scale.

Corresponding author(s): Alexandre C. Siqueira

Last updated by author(s): Apr 4, 2023

Reporting Summary

Nature Portfolio wishes to improve the reproducibility of the work that we publish. This form provides structure for consistency and transparency in reporting. For further information on Nature Portfolio policies, see our [Editorial Policies](#) and the [Editorial Policy Checklist](#).

Statistics

For all statistical analyses, confirm that the following items are present in the figure legend, table legend, main text, or Methods section.

n/a Confirmed

- The exact sample size (n) for each experimental group/condition, given as a discrete number and unit of measurement
- A statement on whether measurements were taken from distinct samples or whether the same sample was measured repeatedly
- The statistical test(s) used AND whether they are one- or two-sided
Only common tests should be described solely by name; describe more complex techniques in the Methods section.
- A description of all covariates tested
- A description of any assumptions or corrections, such as tests of normality and adjustment for multiple comparisons
- A full description of the statistical parameters including central tendency (e.g. means) or other basic estimates (e.g. regression coefficient) AND variation (e.g. standard deviation) or associated estimates of uncertainty (e.g. confidence intervals)
- For null hypothesis testing, the test statistic (e.g. F , t , r) with confidence intervals, effect sizes, degrees of freedom and P value noted
Give P values as exact values whenever suitable.
- For Bayesian analysis, information on the choice of priors and Markov chain Monte Carlo settings
- For hierarchical and complex designs, identification of the appropriate level for tests and full reporting of outcomes
- Estimates of effect sizes (e.g. Cohen's d , Pearson's r), indicating how they were calculated

Our web collection on [statistics for biologists](#) contains articles on many of the points above.

Software and code

Policy information about [availability of computer code](#)

| | |
|-----------------|--|
| Data collection | No custom software or code was used for data collection. |
| Data analysis | All data analysis was performed in the software R (version 4.1.0). The R packages used were: tidyverse (version 1.3.1); ggplot2 (version 3.3.6); ape (version 5.7.1); phytools (version 1.0.3); geiger (version 2.0.9); ggtree (version 3.2.1); cowplot (version 1.1.1); viridis (version 0.6.2); raster (version 3.5.15); parallel (version 4.1.12); XGBoost (version 1.4.1.1); Matrix (version 1.4.0); pdp (version 0.8.1); data.table (version 1.14.2); png (version 0.1.7); grid (version 4.1.2); phangorn (version 2.11.1); bayou (version 2.2.0); mvMORPH (version 1.1.4); PCMBase (version 1.2.12); PCMBaseCpp (version 0.1.9); and PCMFit (version 1.1.0). |

For manuscripts utilizing custom algorithms or software that are central to the research but not yet described in published literature, software must be made available to editors and reviewers. We strongly encourage code deposition in a community repository (e.g. GitHub). See the Nature Portfolio [guidelines for submitting code & software](#) for further information.

Data

Policy information about [availability of data](#)

All manuscripts must include a [data availability statement](#). This statement should provide the following information, where applicable:

- Accession codes, unique identifiers, or web links for publicly available datasets
- A description of any restrictions on data availability
- For clinical datasets or third party data, please ensure that the statement adheres to our [policy](#)

The datasets generated during and/or analyzed during the current study are available at the Zenodo repository (<https://doi.org/10.5281/zenodo.7797270>). There are no restrictions on data availability. The phylogeny used in the main analysis was downloaded from The Fish Tree of Life (<https://fishtreeoflife.org>). Publicly available datasets used in the study include: FishBase (<http://www.fishbase.org>), and the data repository of Morais and Bellwood (<https://doi.org/10.4225/28/5ae8f3cc790f9>). Source data are provided with this paper.

Human research participants

Policy information about [studies involving human research participants and Sex and Gender in Research](#).

Reporting on sex and gender

n/a

Population characteristics

n/a

Recruitment

n/a

Ethics oversight

n/a

Note that full information on the approval of the study protocol must also be provided in the manuscript.

Field-specific reporting

Please select the one below that is the best fit for your research. If you are not sure, read the appropriate sections before making your selection.

Life sciences

Behavioural & social sciences

Ecological, evolutionary & environmental sciences

For a reference copy of the document with all sections, see nature.com/documents/nr-reporting-summary-flat.pdf

Ecological, evolutionary & environmental sciences study design

All studies must disclose on these points even when the disclosure is negative.

Study description

We analysed the evolution of somatic growth across coral reef fishes. We combined extreme gradient boosted regression trees with phylogenetic comparative methods to detect the timing, number, location, and magnitude of shifts in the adaptive regime of somatic growth and body size. We also explored the evolution of the allometric relationship between body size and growth.

Research sample

The research sample was composed of all species of teleost coral reef fishes that had parameters for the calculation of growth available in the literature and FishBase (fishbase.org). The rationale for our sample choice is that we were interested in exploring the evolution of growth across as many coral reef fish species that we could possibly include in the analyses. Most of the data is publicly available through FishBase (see Data collection), the most comprehensive repository for ichthyological data to-date.

Sampling strategy

Sample size was determined by availability of growth parameters and phylogenetic data for coral reef fishes. We used all available data in our study.

Data collection

All data were collected from publicly available online repositories including FishBase (fishbase.org) and FishTreeofLife (fishtreeoflife.org), and published literature.

Timing and spatial scale

The scope of this study is global. Since all data used was publicly available, there were no time constraints for data collection.

Data exclusions

There were no data exclusions.

Reproducibility

Since our study is not an experiment, our analyses do not contain replicates. However, we provide all the relevant data and code to reproduce the results using the same framework that we utilized.

Randomization

This is not relevant to our study, because we did not perform an experiment that required group allocation. Organisms analyzed herein were chosen based on habitat and taxonomic affinities (coral reef fishes).

Blinding

This is not relevant to our study, because we did not perform an experiment that required blinding.

Did the study involve field work? Yes No

Reporting for specific materials, systems and methods

We require information from authors about some types of materials, experimental systems and methods used in many studies. Here, indicate whether each material, system or method listed is relevant to your study. If you are not sure if a list item applies to your research, read the appropriate section before selecting a response.

Materials & experimental systems

- | | |
|-------------------------------------|-------------------------------|
| n/a | Involved in the study |
| <input checked="" type="checkbox"/> | Antibodies |
| <input checked="" type="checkbox"/> | Eukaryotic cell lines |
| <input checked="" type="checkbox"/> | Palaeontology and archaeology |
| <input checked="" type="checkbox"/> | Animals and other organisms |
| <input checked="" type="checkbox"/> | Clinical data |
| <input checked="" type="checkbox"/> | Dual use research of concern |

Methods

- | | |
|-------------------------------------|------------------------|
| n/a | Involved in the study |
| <input checked="" type="checkbox"/> | ChIP-seq |
| <input checked="" type="checkbox"/> | Flow cytometry |
| <input checked="" type="checkbox"/> | MRI-based neuroimaging |